PCN Psychiatry and Clinical Neurosciences

REGULAR ARTICLE

Cefepime-induced encephalopathy: Neural mass modeling of triphasic wave-like generalized periodic discharges with a high negative component (Tri-HNC)

Hidetaka Tamune, MD [1,2,3]* Yu Hamamoto, MD,[1,2] Naofumi Aso, PhD[4,5] and Naoki Yamamoto, MD, PhD[1]

Aim: Cefepime, a fourth-generation cephalosporin, acts as a $GABA_A$ receptor antagonist. Cefepime-induced encephalopathy (CIE) is frequently overlooked. We aimed to clarify the clinical features, characteristic electroencephalography (EEG), and mechanisms of CIE to aid in its early recognition.

Methods: CIE cases documented by a single-center consultation–liaison team between April 2015 and March 2017 were retrospectively reviewed. For further investigation, neural mass modeling was performed *in silico*.

Results: Three patients with CIE refused medication/examination and showed overt pain, palilalia, and much greater deterioration of eye and verbal response than the motor response, which was possibly related to GABAergic dysfunction. Triphasic wave-like generalized periodic discharges with a high negative component (Tri-HNC) were identified on the EEG of all three cases. The simulation reproduced the characteristic feature of 2–3 Hz Tri-HNC and recovery course on EEG, and a possible involvement of individual differences in pharmacological intervention. It also suggested that auto-inhibition (synaptic inputs from interneuron to interneuron) dysregulation contributed to generating Tri-HNC in CIE.

Conclusion: As CIE is iatrogenic and continues unless cefepime is stopped, early recognition is crucial. Physicians should be vigilant about altered mental status, pain, and verbal changes in patients taking cefepime. Tri-HNC on EEG can expedite the diagnosis of CIE, and the association between Tri-HNC and CIE suggests that an excitatory and inhibitory imbalance due to the dysfunction of GABAergic interneurons is the underlying mechanism. This modeling may offer a new method of investigating disorders related to GABAergic dysfunction.

Keywords: *computer simulation, electroencephalography, encephalopathy, GABAergic neurons, non-convulsive status epilepticus.*

http://onlinelibrary.wiley.com/doi/10.1111/pcn.12795/full

Identifying the primary cause of altered mental status is difficult since various confounders are associated with the patient's condition. Although antibiotics are known to cause delirium, this adverse effect is largely under-recognized.[1] Cefepime, a fourth-generation cephalosporin, acts as a $GABA_A$ receptor antagonist[2] and often induces antibiotic-associated encephalopathy.[1] In the intensive care unit, 15% of patients treated with intravenous cefepime for at least 3 days suffer cefepime-induced encephalopathy (CIE), but this condition is frequently overlooked.[3] To aid in its early recognition, we reviewed three cases of CIE presenting unique triphasic wave-like generalized periodic discharges with a high negative component (Tri-HNC).

Generalized periodic discharges (GPD) are commonly encountered in metabolic encephalopathy and cerebral hypoxia[4] and can be simulated using neural mass modeling.[5,6] Synaptic failure or neuronal damage of inhibitory interneurons presumably plays a critical role.[4,7] To improve our understanding of the mechanism underlying CIE, which is presumably related to GABAergic interneuron dysfunction, we performed neural mass modeling to reproduce the Tri-HNC *in silico*.

Methods

Clinical data collection and ethical considerations

Three patients with CIE were referred to the consultation–liaison (C-L) team between April 2015 and March 2017 at Tokyo Metropolitan Tama Medical Center, a 789-bed tertiary care teaching hospital in Tokyo, Japan. The C-L service, which is available around-the-clock, receives approximately 850 patients annually. EEG were recorded for all three patients. Twenty-one electrodes (13 out of 21 for a simplified recording) were placed on the scalp in accordance with the International 10–20 system. The time constant and the high-cut filter were set to 0.3 s and 60 Hz, respectively. We obtained written informed consent from Patients 1 and 2, and the study was approved by the institutional review board at Tokyo Metropolitan Tama Medical Center with a waiver of informed consent from Patient 3 (due to death).

Neural mass modeling

In the simulation, we used a spatially homogeneous version of neural mass modeling, which is basically a mean field model of the cortex.[4–6,8] Figure 1a,b present an overview of the model. The model

[1] Department of Neuropsychiatry, Tokyo Metropolitan Tama Medical Center, Tokyo, Japan
[2] Department of Neuropsychiatry, Graduate School of Medicine, The University of Tokyo, Tokyo, Japan
[3] Department of Cellular Neurobiology, Graduate School of Medicine, The University of Tokyo, Tokyo, Japan
[4] Department of Earth and Planetary Science, Graduate School of Science, The University of Tokyo, Tokyo, Japan
[5] School of Science, Tokyo Institute of Technology, Tokyo, Japan
* Correspondence: Email: tamune-tky@umin.ac.jp

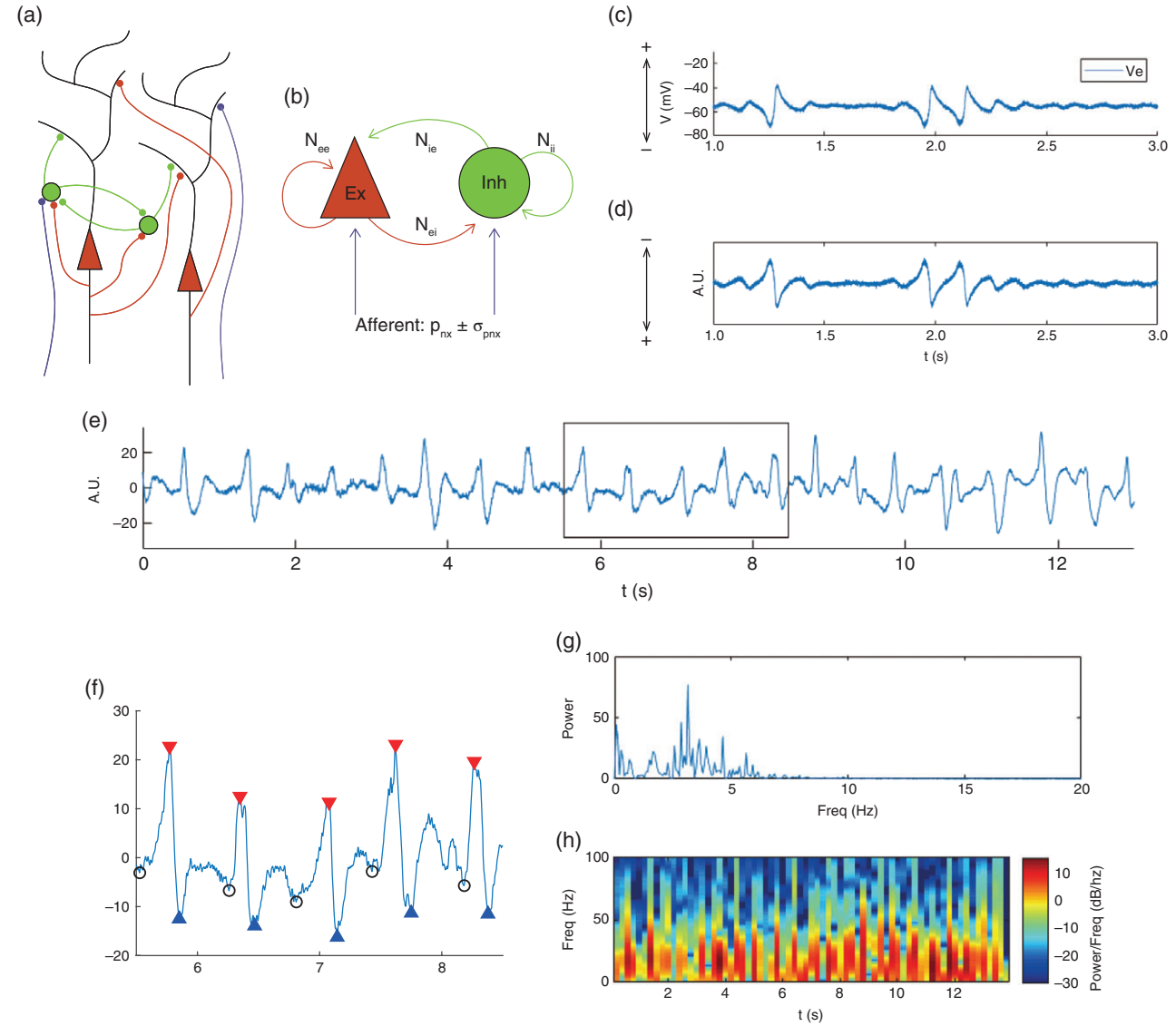

Fig.1 An overview of the mean field model, simulation, and analysis. (a) From the cortical circuitry comprised of excitatory and inhibitory neurons, (b) only one excitatory neuron (Ex) and one inhibitory neuron (Inh) are extracted for the mean field model. Both excitatory and inhibitory neurons receive input via intracortical synaptic projections (Ex->Ex, Ex->Inh, Inh->Ex and Inh->Inh) as well as nonspecific excitatory input from regions not explicitly incorporated into the model, such as the thalamus ($p \pm \sigma$). N_{kx} denotes the number of synaptic inputs from k to x. The indices e and i refer to the excitatory, and inhibitory neurons, respectively. Using the values of N_{kx}, the model generates the mean voltage of the excitatory and inhibitory neurons. (c) The mean voltage of the excitatory neuron (N_{ex} = 3000, N_{ix} = 380). (d) To illustrate the simulated scalp electroencephalography (EEG), the plus and minus ends were simply reversed and arbitrary units were used for the *y*-axis. (e) Using normalized EEG, (f) negative/positive ratio, complex frequency, and complex duration were calculated. (g) The power of the waves and (h) spectrogram are also presented.

describes the dynamics of the average membrane potentials of a cortical macrocolumn comprised of excitatory (pyramidal) neurons and GABAergic inhibitory (inter-)neurons. In short, both excitatory and inhibitory neurons receive input via intracortical synaptic projections as well as nonspecific excitatory input from regions not explicitly incorporated into the model, such as the thalamus. The excitatory neurons excite both themselves and the inhibitory interneurons through glutamate-mediated synapses. The interneurons inhibit both themselves and the excitatory neurons through GABA-mediated synapses.[4,7]

Model parameters and equations

The indices e and i used below refer to the excitatory and inhibitory neurons, respectively. The membrane potentials are denoted by $V_k(t)$ for k = e,i. Their dynamics are governed by the following set of differential equations:

$$\tau_e \frac{dV_e}{dt} = V_e^{\text{rest}} - V_e(t) + \Psi^e_{\text{AMPA}} I_{ee}(t) + \Psi^e_{\text{GABA}} I_{ie}(t) + \Psi^e_{\text{AMPA}} I_{ne}(t),$$

$$\tau_i \frac{dV_i}{dt} = V_i^{\text{rest}} - V_i(t) + \Psi^i_{\text{AMPA}} I_{ei}(t) + \Psi^i_{\text{GABA}} I_{ii}(t) + \Psi^i_{\text{AMPA}} I_{ni}(t),$$

where τ_k and V_k^{rest} denote the membrane time-constants and resting-potentials, respectively, and I_{kx} is proportional to the current flowing into population x due to the activity of population k. The currents I_{ne} and I_{ni} model the afferent, non-specific input to the cortical column, and are modeled as uncorrelated white-noise processes with the mean values p_{ne} and p_{ni} and the standard deviations $\sigma_{p_{ne}}$ and $\sigma_{p_{ni}}$, respectively. The currents I_{kx} are given by

$$I_{kx}(t) = h_{\text{AMPA/GABA}} \otimes N_{kx} S_k(V_k(t)),$$

PCN Psychiatry and Clinical Neurosciences

where $h_{AMPA/GABA}(t) = tH_{AMPA/GABA}\gamma_{AMPA/GABA}\exp(1-\gamma_{AMPA/GABA}t)$ is the response function of AMPA/GABAergic receptors located on the dendrites of neurons within population x. N_{kx} denotes the number of synaptic inputs from k to x, which is a variable in this study. The function S_k relates the membrane potential of population k to its firing-rate, and is given by

$$S_k(V_k) = \frac{Q_k^{max}}{1+\exp\left(-\frac{\sqrt{2}\left(V_k(t)-V_k^{spike}\right)}{\sigma_k}\right)}.$$

The variables $\Psi^k_{AMPA/GABA}$ are dimensionless and model the dependence of AMPA/GABAergic synaptic conductance on the membrane potential of the post-synaptic neural population k. They are given by

$$\Psi^k_{AMPA/GABA}(V_k) = \frac{E_{AMPA/GABA}-V_k(t)}{|E_{AMPA/GABA}-V_k^{rest}|}.$$

The baseline values for all model parameters were modified from previous reports[5] and are listed in Table 1. For further details, see Tjepkema-Cloostermans *et al*.[6]

Illustrating EEG, *in silico* analysis, and statistics

With the values of N_{kx}, the model generated the mean voltage of the excitatory and inhibitory neurons. To illustrate the simulated scalp EEG, the plus and minus ends were simply reversed, and arbitrary units were used for the *y*-axis (Fig. 1c,d).

One representative recording of real or simulated EEG was normalized to its amplitude (Fig. 1e). We defined the negative/positive ratio as the amplitude ratio of negative component over positive component of each GPD. We also defined the complex frequency and the complex duration as the number of GPD shown per second and the duration of each GPD, respectively, based on peak-to-peak interval times using semi-automatic peak detection (Fig. 1f). We characterized spectral components based on fast Fourier transform (FFT). In detail, we computed the power spectrum of the whole waveform, to visualize overall characteristics (Fig. 1g), and spectrogram using half-overlapping 0.4-s time windows with a hamming window to visualize temporal variation (Fig. 1h) on MATLAB (R2018a, MathWorks, Inc., Natick, MA, USA), with a signal processing toolbox. Negative/positive ratio, complex frequencies, and complex duration were tested using Welch's analysis of variance on MATLAB. $P < 0.05$ was considered statistically significant.

Table 1. Model parameters, their symbols, and baseline values

Parameter	Symbol	Baseline value
Maximum spike-rate	Q_k^{max}	500 s^{-1}
Spike-threshold	V_k^{spike}	−60 mV
SD of spike-threshold	σ_k	5 mV
Synaptic efficacy	H_{GABA}, H_{AMPA}	0.71 mV
Reversal potential	E_{GABA}, E_{AMPA}	−90, 40 mV
Number of synaptic inputs from k to x	N_{ei}, N_{ee}, N_{ie}, N_{ii}	3000, 3000, 500, 500 (variable)
Membrane time-constant	τ_e, τ_i	0.094, 0.042 s
Resting potential	V_k^{rest}	−70 mV
Synaptic rate-constant	γ_{GABA}, γ_{AMPA}	65, 300 s^{-1}
Non-specific firing rate	p_{ne}, p_{ni}	3460, 5070 s^{-1}
SD of non-specific fluctuation	$\sigma_{p_{ne}}$, $\sigma_{p_{ni}}$	1000, 150 s^{-1}

The indices k and x refer to neural populations of type k and x for e (excitatory-) and i (inhibitory-) neurons

Results

Case presentations

Case 1 was that of a 64-year-old woman on dialysis. Four days after cefepime was started, she suddenly began refusing medication and repeatedly complained about feeling pain with 'ouch, ouch, ouch…'. Delirium was suspected, and the patient was referred to our C-L team. Her Glasgow Coma Scale was E2V3M4, and her EEG showed 2–3 Hz Tri-HNC (Day 1, Fig. 2a). Other diseases causing altered mental status were excluded as possible by close examinations. We recommended that cefepime be stopped and that the patient be observed closely without any additional interventions, such as benzodiazepines or anti-epileptic drugs. Four days after the consultation, her mental status normalized, and her EEG showed an alpha rhythm with waves of various frequencies (Day 5, Fig. 2b). After she became fully alert, a follow-up EEG showed no epileptic discharges (Days 12 and 31; Fig. 2c,d, respectively). Figure 2e shows the spectrogram throughout the clinical course. Alpha-band oscillation recovered clearly by Day 31.

Case 2 was that of a 44-year-old man who experienced E1V2M4 and incontinence and refused to be examined. Case 3 involved a 94-year-old woman who experienced E1V2M4 and pain and refused medication. All three patients were cared for in a non-intensive care unit setting and showed palilalia. Myoclonus was not noticed by patients themselves or staff. Their clinical course is summarized in Table 2, and the EEG in Cases 2 and 3 are shown in Figure 2f–i and Figure 2j, respectively. The spectrograms taken throughout the clinical course in Cases 2 and 3 are shown in Figure 2k,l.

Neural mass modeling

To examine the underlying mechanism, we performed a simulation using neural mass modeling.

Simulation of Tri-HNC and the recovery course in CIE

We first used the same number for N_{ii} and N_{ie} (represented as N_{ix}) in accordance with the original Liley model.[5] To simulate cefepime-induced neurotoxicity as $GABA_A$ receptor antagonism, N_{ix} was decreased from 500 (100% input). As expected, $N_{ix} = 380$ (76% input) partly explained the characteristic feature of Tri-HNC (Fig. 3a) while the FFT indicated the dominant frequency to be 6–7 Hz (Fig. 3b). Figure 3c shows a spectrogram corresponding to Figure 3a.

To assess the recovery course, N_{ix} was changed from 380 in a stepwise fashion to 500. Figure 3d shows the simulated EEG at $N_{ix} = 500$ (100% input). The power for each frequency (from left to right) is illustrated in Figure 3e. The dominant background activity changed from 7 Hz ($N_{ix} = 380$, 76% input) to 12 Hz ($N_{ix} = 500$, 100% input). The spectrograms near the phase-transition point (Fig. 3f) qualitatively reproduced the clinical recovery course (Fig. 2e).

Simulation of pharmacological intervention

Benzodiazepines, such as clonazepam and diazepam, are frequently used for alleviating CIE; however, their effectiveness has not been proven and may vary in individual cases.[9–13] To investigate the effect of pharmacological intervention, we fixed N_{ix} at 380 as a constant and moved N_{ex} ($=N_{ee} = N_{ei}$) simultaneously from 1500 to 3000, since some interneurons are insensitive to benzodiazepines.[14,15] At $N_{ex} = 1500$ or 1800 (50% or 60% input, respectively), the simulated EEG showed a low voltage pattern (Fig. 4a,b). Although they showed alpha-band oscillations at $N_{ex} = 2100$, 2400, and 2700 (70%, 80%, and 90% input in Fig. 4c–e, respectively), strikingly, they became unstable again at $N_{ex} = 3000$ (100% input, Fig. 4f), suggesting that pharmacological intervention had transient effects and that the permanent recovery of N_{ix} played a critical role in stability.

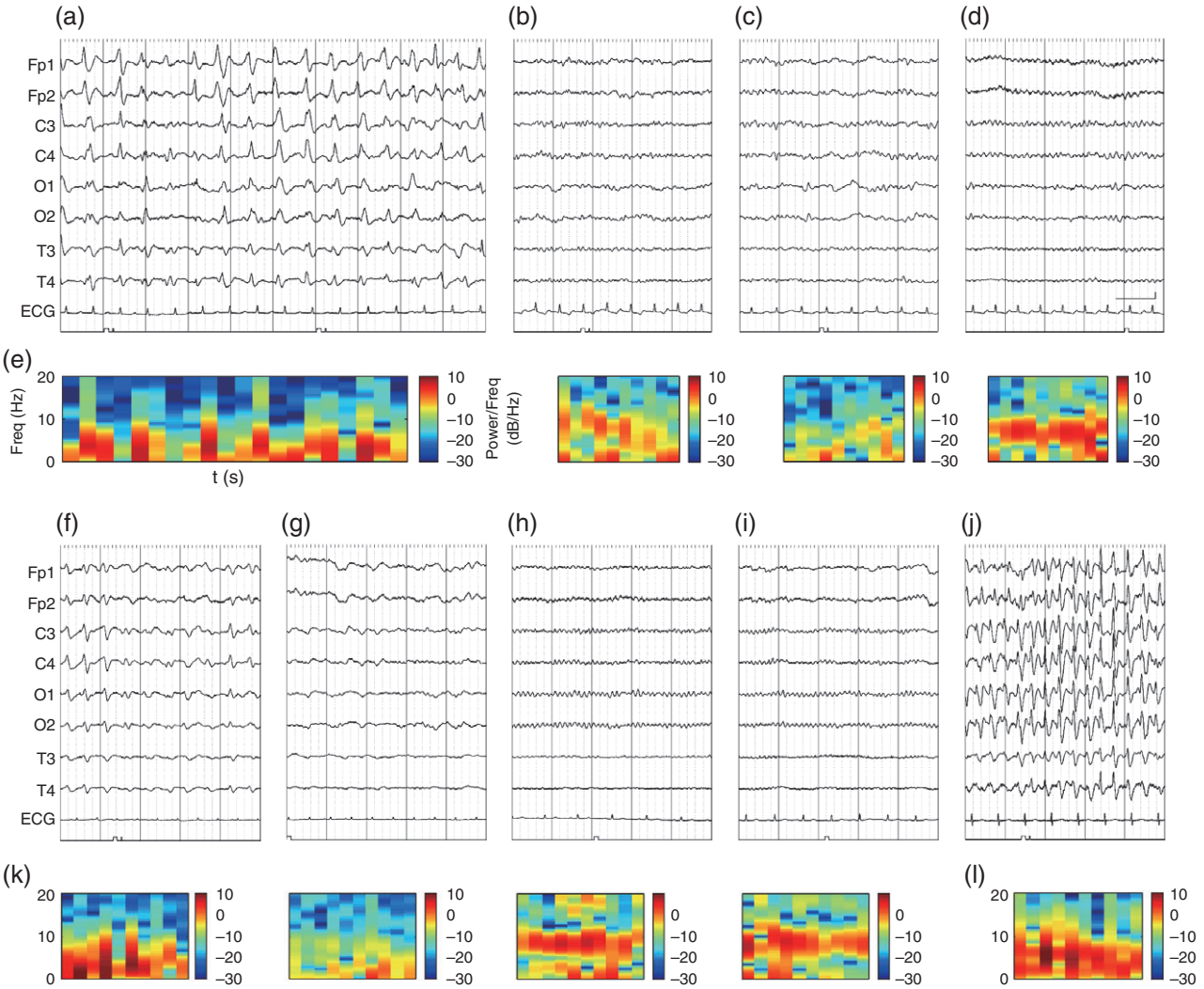

Fig.2 Monopolar electroencephalography (EEG) during the clinical course of cefepime-induced encephalopathy. (a–d) Case 1, a 64-year-old woman on dialysis. (a) Unique 2–3 Hz triphasic wave-like generalized periodic discharges with a high negative component (Tri-HNC) are shown (Consultation Day 1). (b) After cessation of cefepime, her mental status recovered, and her EEG showed an alpha rhythm with waves of various frequencies (Day 5). Follow-up EEG showed no epileptic discharges on (c) Day 12 or (d) Day 31. Scale: 1 s, 50 μV. (e) The spectrograms throughout the clinical course of Case 1. Alpha-band oscillation had recovered clearly by Day 31. (f–i) Case 2, a 44-year-old man. EEG taken on consultation Days 1, 3, 15, and 288 (after discharge) are shown. (j) Case 3, a 94-year-old woman. EEG taken on consultation Day 1. All three cases represent Tri-HNC. (k,l) The spectrograms throughout the clinical courses of Cases 2 and 3.

Table 2. Summary of three cases of cefepime-induced encephalopathy

Age (years)	Sex	Weight (kg)	eGFR	Adjusted for renal function	Indication	Clinical findings	Latency (days)	Intervention	Days to improvement
64	Female	52.7	21 (on dialysis)	No	Infectious endocarditis	AMS (E2V3M4), pain, palilalia, refusal of medication	4	Observation	4
44	Male	40.0	33	No	Pneumonia	AMS (E1V2M4), palilalia, refusal of examination	5	Observation	4
94	Female	38.3	14	Yes	Cholangitis, cellulitis	AMS (E1V2M4), pain, palilalia, refusal of medication	4	DZP, PHT	4

AMS, altered mental status; eGFR, estimated glomerular filtration rate (mL/min/1.73m^2); DZP, diazepam 5 mg; PHT, phenytoin 250 mg.

This simulation was consistent with clinical observations and led us to form the hypothesis that the underlying mechanism involved the induction of low-voltage EEG activity in the CIE patient by high-dose benzodiazepine while low-dose (or an appropriate concentration of) benzodiazepine transiently improved awareness without maintaining full-recovery until sufficient cefepime clearance.

PCN Psychiatry and Clinical Neurosciences

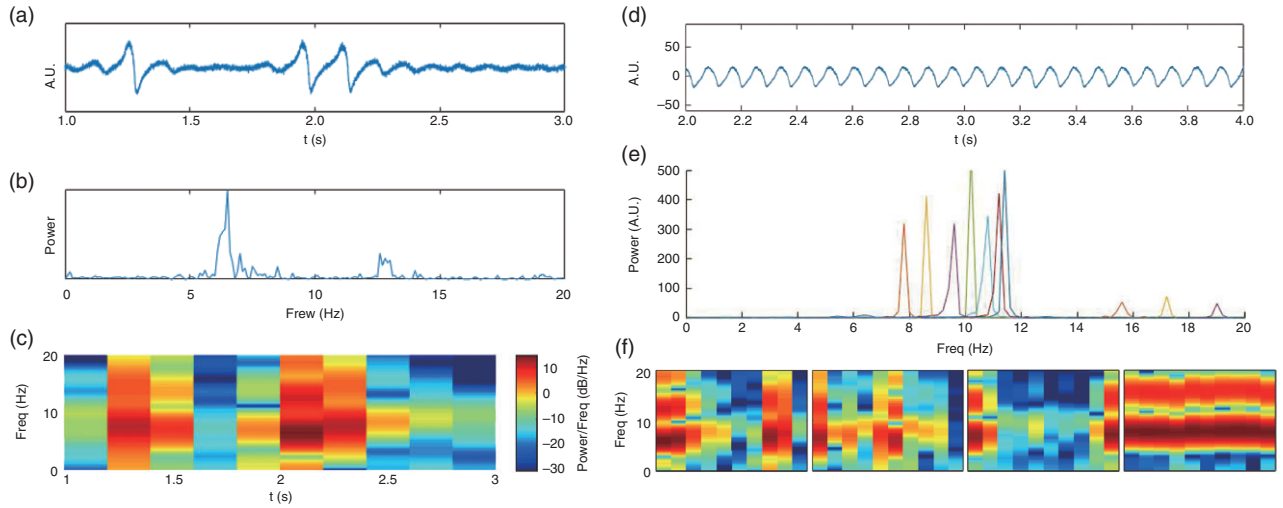

Fig.3 Simulation of triphasic wave-like generalized periodic discharges with a high negative component (Tri-HNC) and recovery course on electroencephalography (EEG). (a) Simulated EEG explains the characteristic feature of 2–3 Hz Tri-HNC (on N_{ix} = 380, 76% input), while (b) fast Fourier transform indicates that the dominant frequency was 6–7 Hz. (c) A spectrogram corresponding to (a). (d) The simulated EEG at N_{ix} = 500 (100% input). (e) Illustration of the power of each frequency component (from left to right: N_{ix} = 380, 390, 400, 420, 440, 460, 480, and 500). The dominant background activity changed from 7 Hz (N_{ix} = 380, 76% input) to 12 Hz (N_{ix} = 500, 100% input). (f) The spectrograms near the phase-transition point (N_{ix} = 380, 381, 382, 390) qualitatively reproduced the clinical recovery course.

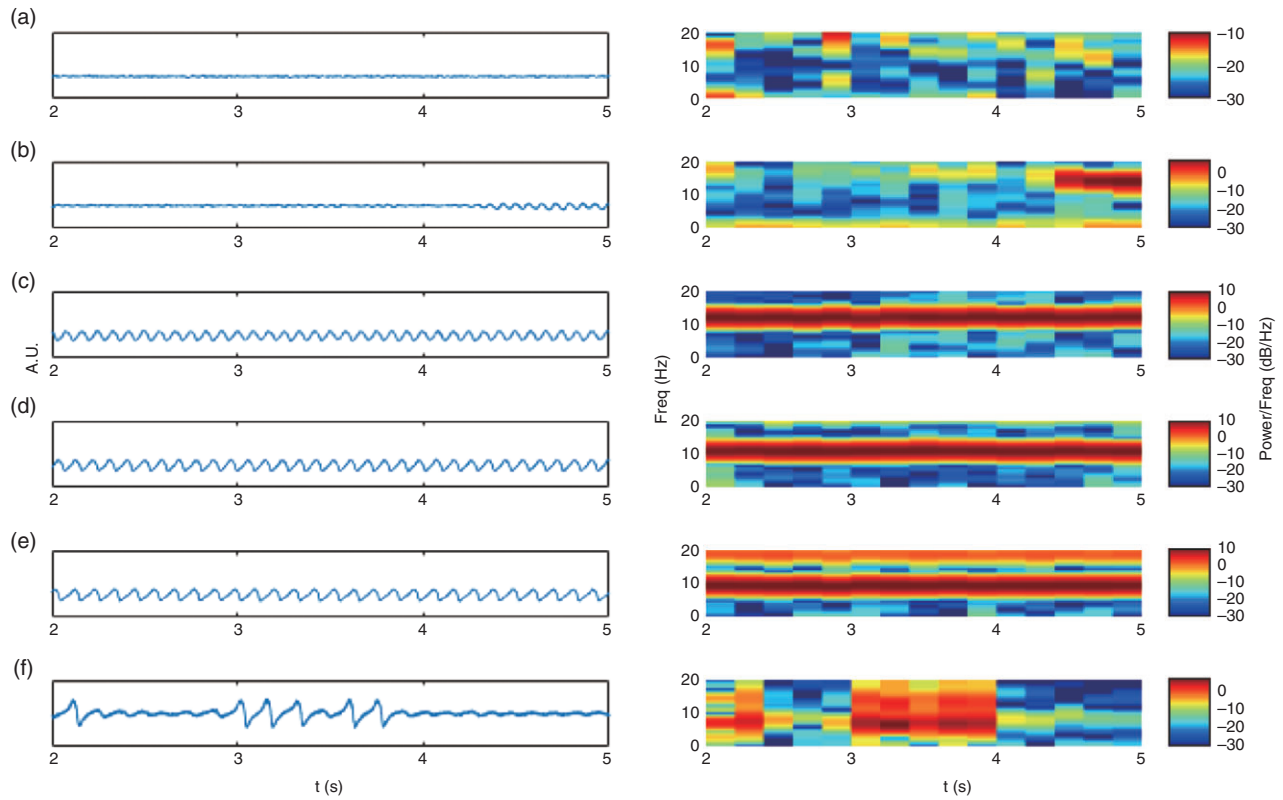

Fig.4 Simulation of pharmacological intervention. (a,b) With N_{ix} = 380 as a constant, the simulated electroencephalography (EEG) showed a low-voltage pattern at N_{ex} = 1500 or 1800 (50% and 60% input, respectively), while (c–e) they showed alpha-band oscillations at N_{ex} = 2100, 2400, and 2700 (70%, 80%, and 90% input, respectively). (f) Notably, the EEG pattern became unstable again at N_{ex} = 3000 (100% input). These findings indicate individual pharmacological differences.

Excitatory and inhibitory imbalance explains the characteristic features seen on the EEG

We hypothesized that excitatory and inhibitory (E/I) imbalance was essential to explaining the features seen on the EEG. To determine which parameter was chiefly responsible for these characteristic features, we conducted stepwise parameter studies *in silico.*

First, we set N_{ix} at 500 (100% input, constant) and experimentally changed N_{ee} and N_{ei} individually from 1200 to 6000 (40% to 200% input; Fig. 5a). This simulation suggested that alpha-band oscillation was robust in the condition that both N_{ee} and N_{ei} were under 100% input and that N_{ee} basically provided the dominant frequency. It also suggested that N_{ee} and N_{ei} balance was a key factor of

phase-transition, as previously reported.[6,7] As expected, the Tri-HNC patterns can be generated at N_{ee} = 4650 and N_{ei} = 5850 (Fig. 6a), which indicated that increased E/I was essential to generate the Tri-HNC.

Cefepime theoretically antagonizes GABAergic inhibitory inputs. To determine whether N_{ie} or N_{ii} contributed more to generating GPD, we set N_{ex} = 3000 (100% input, constant) and changed N_{ie} and N_{ii} individually from 280 to 500 (56% to 100% input, Fig. 5b). This simulation suggested that N_{ie} provided the dominant frequency and that N_{ie} and N_{ii} balance was another key factor of phase-transition, indicating that only N_{ie} or N_{ii} was not enough to generate GPD. Moreover, the 2–3 Hz Tri-HNC pattern was most closely reproduced at N_{ie} = 350 and N_{ii} = 292 (Fig. 6b).

To investigate another possibility that inputs to interneuron is the underlying mechanism, we set N_{ee} = 3000 (100% input, constant) and N_{ie} = 500 (100% input, constant) and changed N_{ei} and N_{ii} individually as shown in Figure 5c; however, the dominant frequencies were restricted to the alpha-band and GPD were not able to be reproduced with any of the parameters. This finding is similar in N_{ie} and N_{ii} stepwise study under N_{ei} and N_{ii} constant (data not shown). These findings demonstrated that only one parameter was insufficient to explain the GPD and that alpha-band oscillation was robust enough to overcome the external disturbance.

We also examined a possible application of neural mass modeling. With appropriate parameters, neural mass modeling generated characteristic features, such as Tri-HNC at another frequency (Fig. 6c) and spindle (Fig. 6d). These simulations suggested that E/I balance accounted for some of the characteristic features seen on the EEG.

Finally, we quantitatively compared the negative/positive ratio, complex frequencies, and complex durations of real and simulated EEG. Negative/positive ratios (Fig. 6e) did not differ statistically, whereas the complex frequencies (Fig. 6f) and the complex durations (Fig. 6g) differed statistically. The findings were based on a small number of cases and await validation by further studies.

Discussion

Clinical presentation

We noticed that 2–3 Hz GPD with a high negative component (above baseline) seemed to characterize cefepime-induced encephalopathy[9–12,16–18] in contrast to the triphasic waves induced by other illnesses, such as hepatic encephalitis[10] or Creutzfeldt–Jakob disease.[19] Moreover, the triphasic morphology with negative polarity in the dominant phase was perceived as differing from the 'typical' triphasic wave by clinicians (odds ratio: 0.09, 0.02–0.22),[20] suggesting that the clinicians differentiated the Tri-HNC from 'typical' triphasic wave; however, only a few studies have focused on this characteristic feature.[10,21]

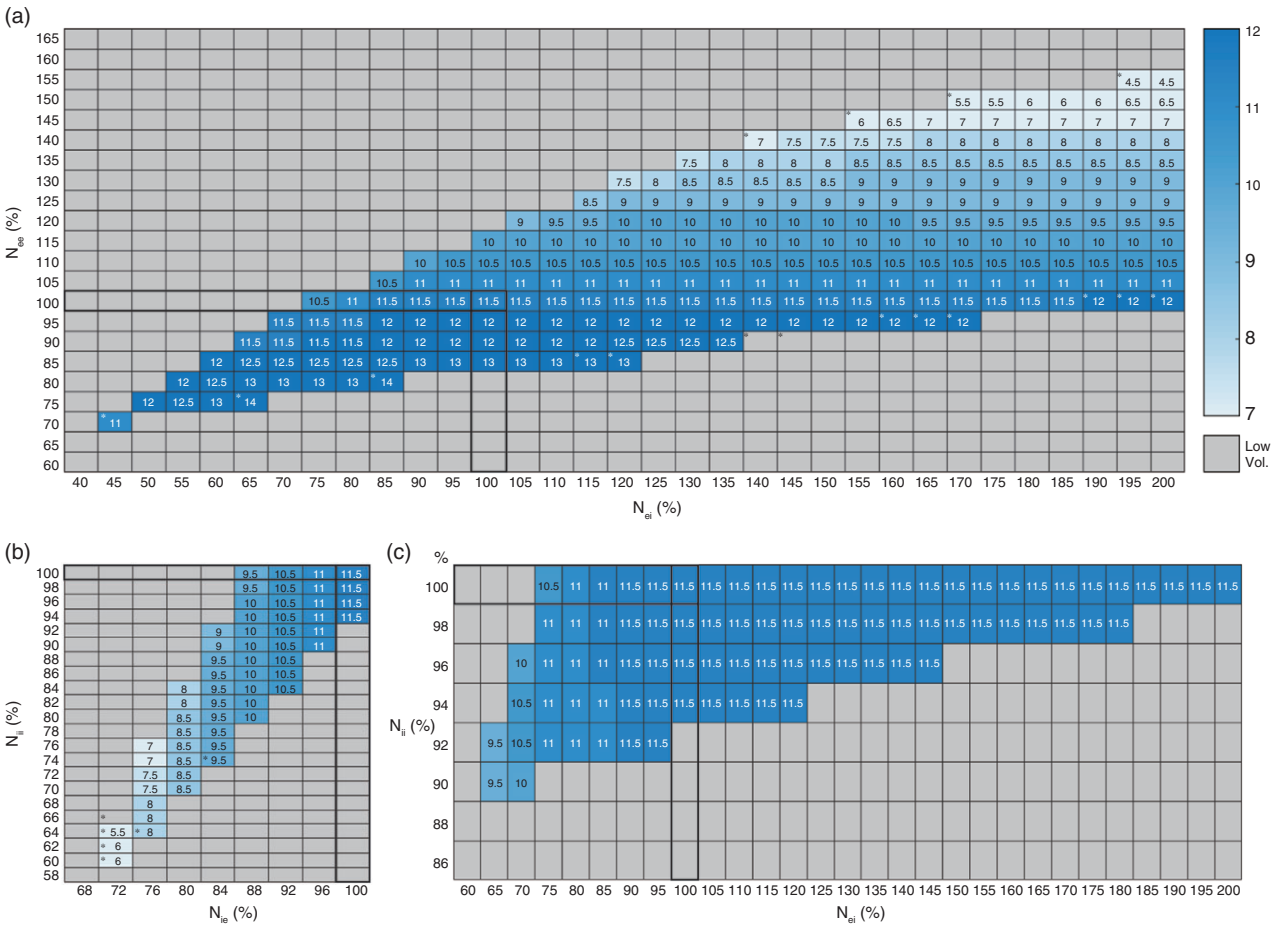

Fig.5 Dominant frequencies and phase-transition experimentally simulated using each excitatory and inhibitory parameter. (a) N_{ei} from 1200 to 6000 (40% to 200% input) and N_{ee} from 1800 to 4950 (60% to 165% input) under N_{ix} constant (500, 100% input), suggesting that N_{ee} provided the dominant frequency and that N_{ee} and N_{ei} balance was a key factor of phase-transition. (b) N_{ie} from 340 to 500 (68% to 100% input) and N_{ii} from 290 to 500 (58% to 100% input) under N_{ex} constant (3000, 100% input), suggesting that N_{ie} provided the dominant frequency and that N_{ie} and N_{ii} balance was another key factor of phase-transition. (c) N_{ei} from 1800 to 6000 (60% to 200% input) and N_{ii} from 430 to 500 (86% to 100% input) under N_{ee} and N_{ie} constant (100% input), indicating that N_{ii} and N_{ei} were insufficient to explain the generalized periodic discharge generation, and that alpha-band oscillation was robust enough to overcome the external disturbance. Low Vol., low voltage EEG. *Phase-transition point.

Psychiatry and Clinical Neurosciences published by John Wiley & Sons Australia, Ltd on behalf of Japanese Society of Psychiatry and Neurology

Psychiatry and Clinical Neurosciences 73: 34–42, 2019

PCN Psychiatry and Clinical Neurosciences

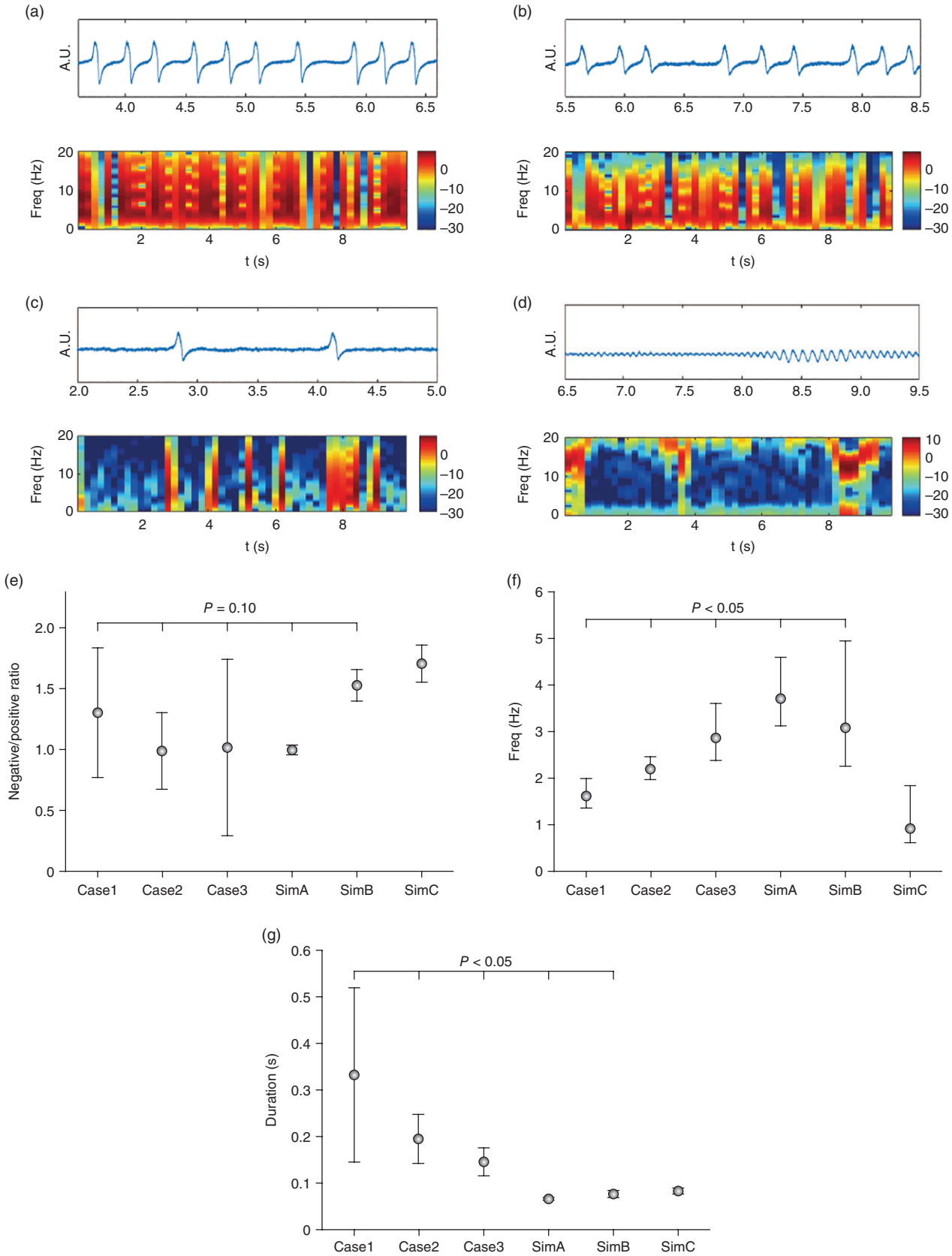

Fig.6 Simulation of other characteristic features and statistics. (a,b) A unique 2–3 Hz triphasic wave-like generalized periodic discharges with a high negative component (Tri-HNC) pattern similar to that seen in cefepime-induced encephalopathy was reproduced with certain parameters. (a) N_{ee} = 4650, N_{ei} = 5850, and N_{ix} = 500. (b) N_{ex} = 3000, N_{ie} = 350, and N_{ii} = 292. (c) Tri-HNC with another frequency (N_{ee} = 4500, N_{ei} = 5100, N_{ix} = 500) and (d) spindle (N_{ee} = 2700, N_{ei} = 4500, N_{ix} = 500) was also generated. (e) The negative/positive ratios (P = 0.10) did not differ statistically between the clinical cases and simulations, whereas (f) complex frequencies and (g) complex durations differed statistically (P < 0.05). Error bars indicate SD.

We identified Tri-HNC in all three C-L cases of CIE with chronic kidney disease (Fig. 2 and Table 2). Latency and days to improvement were almost the same as those previously reported,[1,22] and other diseases causing altered mental status were carefully excluded in all the cases. All the patients showed a similar, characteristic clinical course (Table 2), including refusal of medication/examination, complaints of overt pain and palilalia, and much greater deterioration of eye and verbal response than the motor response. Previous reports showed that patients with CIE presented altered mental status[22] more often than seizures[23,24] or psychotic symptoms.[1] Although it is still unclear when antibiotic-associated altered mental status with GPD should be diagnosed as non-convulsive status epilepticus,[25] the characteristic clinical presentations in the present cases led the physicians to assume a psychological cause. Interestingly, previous reports suggested that aphasia was a diagnostic feature of CIE,[17,18,23] and we hypothesized that palilalia was a mild sign of aphasia in patients with CIE. A previous study showed that memory formation, sensory processing, and pain were cognitive functions associated with GABAergic inhibition.[26] Together with the evidence that cefepime acts as a $GABA_A$ receptor antagonist, the symptoms that the patients experienced can be summarized to be dysfunctions of GABAergic inhibition.

Neural mass modeling and the relevance of Tri-HNC detection

Our neural mass modeling reproduced the Tri-HNC and a characteristic feature seen on EEG in the course of recovery (Fig. 3) and suggested a potential mechanism for individual differences in patients' responses to pharmacological interventions (Fig. 4). *In silico* analysis revealed that generating GPD was a circuit-level phenomenon and offered some hints regarding the relation between alpha-band oscillation and awareness (Fig. 5). Together with the biological insight, it also suggested that the number of synaptic inputs from interneuron to interneuron (N_{ii}, auto-inhibition) dysregulation contributed to generating Tri-HNC in CIE, although auto-inhibition dysregulation alone cannot explain the whole phenomena.

Based on the simulation of pharmacological intervention (Fig. 5), low-dose (or an appropriate concentration of) benzodiazepine can transiently improve awareness; however, sufficient cefepime clearance was suggested to be a requirement for full-recovery. Comparison with a large clinical information dataset is necessary for clarifying whether further pharmacological treatment has long-term benefit and/or side-effect.

A previous case report showed that flumazenil, a $GABA_A$ receptor antagonist, improved the triphasic waves caused by hepatic encephalopathy.[27] We hypothesized that these different types of triphasic wave reflected essentially different activities of the brain. Although our neural mass modeling cannot provide a hypothesis as to which subtype of interneuron, such as PV, SST, or 5HT3aR,[28] plays a key role, it emphasized the importance of the auto-inhibitory system associated with interneuron microcircuits.[29]

Qualitatively and quantitatively, the Tri-HNC had a blunt ascent and descent with a high negative component, relatively long complex duration (indicating triphasic waves rather than a generalized spike–wave complex[25]), and 2–3 Hz complex frequencies (Fig. 6e–g). Of note, we succeeded in simulating the most prominent feature, high negative component, quantitatively (Fig. 6e). The psychological clinical presentations (verbal changes, response to stimuli, and fluctuating attention) and the lack of a need for additional interventions showed that Tri-HNC differed from epileptic discharges and may require a new designation[25] although the matter remains controversial.

To explore other possible applications of neural mass modeling, we simulated the EEG of other disorders related to the dysfunction of GABAergic interneurons. We were able to generate a 0.5–1 Hz Tri-HNC similar to that seen in some patients with glutamic acid decarboxylase antibody-associated encephalitis, who showed 0.3–0.5 Hz Tri-HNC[30,31] (Fig. 6c). It is possible, at any rate, that Tri-HNC is common to various cases of GABAergic interneuron instability. Unfortunately, our neural mass modeling was not able to reproduce 'typical' triphasic waves observed in hepatic encephalopathy, which suggested that some metabolic encephalopathies might not be approximated by the simplified mean field model of synaptic networks. Nonetheless, computational modeling may contribute to clarifying its pathophysiology and offer a new method for investigating disorders related to GABAergic dysfunction.[32]

Limitations

We are aware of several limitations to this study. First, not all patients referred to the C-L team for consultation underwent an EEG examination. Although all three patients presented Tri-HNC, it is possible that other patients with CIE were overlooked as often happens in cases of delirium. Second, the number of cases was too small to draw any firm conclusions about the clinical course. Further, comprehensive, prospective studies are needed for clinical investigation.

Next, neural mass modeling was aimed for an approximation of spatially and temporally homogenous EEG. In the model, the interactions between excitatory and inhibitory neurons are averaged over the whole brain and only one excitatory neuron and one inhibitory neuron with their interactions represent the networks. Relatively complicated concepts, such as the dipole moment or source and sink, are not incorporated into the model; however, Tri-HNC may be one of the best-matched patterns in this simplified model given its spatially and temporally homogenous pattern in the real EEG. A more sophisticated model could reproduce the 'typical' triphasic wave, while our simplified model is just enough to reproduce Tri-HNC.

This study identified a connection between the features of real EEG and neural mass modeling-simulated EEG, suggesting that E/I imbalance due to the dysfunction of GABAergic interneurons was the underlying mechanism of CIE (Fig. S1). As theoretical molecular mechanisms remain speculative at best, further biological experiments are needed to verify our hypothesis.

Conclusion

As CIE is iatrogenic and potentially self-limiting only when cefepime is stopped, early recognition of the symptoms is crucial. In addition to the US Food and Drug Administration recommendation to be aware of the risk of seizures and to recognize the need for dose adjustments when using cefepime,[33] physicians also need to be more vigilant in regards to altered mental status, pain, and verbal changes in patients taking cefepime.

Neural mass modeling reproduced Tri-HNC, a characteristic feature of EEG in patients with CIE. Together with the clinical presentations, Tri-HNC can expedite the diagnosis of CIE. The association between CIE and Tri-HNC suggested that E/I imbalance due to the dysfunction of GABAergic interneurons is the underlying mechanism of CIE. This modeling may offer a new method for investigating disorders related to GABAergic dysfunction.

Acknowledgments

We thank Dr. Teiichi Onuma, Dr. Shigeo Okabe, Dr. Shunsuke Mizutani, Dr. Go Taniguchi, and his team for valuable discussions, Mr. James Robert Valera for his assistance in editing this manuscript, and all the staff for their care of the patients and contributions to this study.

Disclosure statement

The authors have no conflicts of interest to disclose.

Author contributions

H.T. conceived the study. H.T., Y.H., and N.Y. collected the data. H.T. and N.A. analyzed the data. H.T. drafted the first manuscript. All the authors critically revised the manuscript for intellectual content and approved the final version.

Psychiatry and Clinical Neurosciences published by John Wiley & Sons Australia, Ltd on behalf of Japanese Society of Psychiatry and Neurology

Psychiatry and Clinical Neurosciences 73: 34–42, 2019

References

1. Bhattacharyya S, Darby RR, Gonzalez LN, Berkowitz AL. Antibiotic-associated encephalopathy. *Neurology* 2016; **86**: 963–971.
2. Sugimoto M, Uchida I, Mashimo T *et al*. Evidence for the involvement of GABAA receptor blockade in convulsions induced by cephalosporins. *Neuropharmacology* 2003; **45**: 304–314.
3. Fugate JE, Kalimullah EA, Hocker SE, Clark SL, Wijdicks EF, Rabinstein AA. Cefepime neurotoxicity in the intensive care unit: A cause of severe, underappreciated encephalopathy. *Crit. Care* 2013; **17**: R264.
4. van Putten MJAM, Hofmeijer J. Generalized periodic discharges: Pathophysiology and clinical considerations. *Epilepsy Behav.* 2015; **49**: 228–233.
5. Liley DTJ, Cadusch PJ, Dafilis MP. A spatially continuous mean field theory of electrocortical activity. *Network: Comput. Neural Syst.* 2002; **13**: 67–113.
6. Tjepkema-Cloostermans MC, Hindriks R, Hofmeijer J, van Putten MJAM. Generalized periodic discharges after acute cerebral ischemia: Reflection of selective synaptic failure? *Clin. Neurophysiol.* 2014; **125**: 255–262.
7. Ruijter BJ, Hofmeijer J, Meijer HGE, van Putten MJAM. Synaptic damage underlies EEG abnormalities in postanoxic encephalopathy: A computational study. *Clin. Neurophysiol.* 2017; **128**: 1682–1695.
8. Ponten SC, Tewarie P, Slooter AJC, Stam CJ, van Dellen E. Neural network modeling of EEG patterns in encephalopathy. *J. Clin. Neurophysiol.* 2013; **30**: 545–552.
9. Jallon P, Fankhauser L, Du Pasquier R *et al*. Severe but reversible encephalopathy associated with cefepime. *Neurophysiol. Clin.* 2000; **30**: 383–386.
10. Martinez-Rodriguez JE, Barriga FJ, Santamaria J *et al*. Nonconvulsive status epilepticus associated with cephalosporins in patients with renal failure. *Am. J. Med.* 2001; **111**: 115–119.
11. Fernández-Torre JL, Martínez-Martínez M, González-Rato J *et al*. Cephalosporin-induced nonconvulsive status epilepticus: Clinical and electroencephalographic features. *Epilepsia* 2005; **46**: 1550–1552.
12. Grill MF, Maganti R. Cephalosporin-induced neurotoxicity: Clinical manifestations, potential pathogenic mechanisms, and the role of electroencephalographic monitoring. *Ann. Pharmacother.* 2008; **42**: 1843–1850.
13. Thabet F, Al Maghrabi M, Al Barraq A, Tabarki B. Cefepime-induced nonconvulsive status epilepticus: Case report and review. *Neurocrit. Care* 2009; **10**: 347–351.
14. Rudolph U, Crestani F, Benke D *et al*. Benzodiazepine actions mediated by specific gamma-aminobutyric acid(A) receptor subtypes. *Nature* 1999; **401**: 796–800.
15. Bacci A, Rudolph U, Huguenard JR, Prince DA. Major differences in inhibitory synaptic transmission onto two neocortical interneuron subclasses. *J. Neurosci.* 2003; **23**: 9664–9674.
16. Dixit S, Kurle P, Buyan-Dent L, Sheth RD. Status epilepticus associated with cefepime. *Neurology* 2000; **54**: 2153–2155.
17. Sonck J, Laureys G, Verbeelen D. The neurotoxicity and safety of treatment with cefepime in patients with renal failure. *Nephrol. Dial. Transplant.* 2008; **23**: 966–970.
18. Isitan C, Ferree A, Hohler AD. Cefepime induced neurotoxicity: A case series and review of the literature. *eNeurologicalSci* 2017; **8**: 40–43.
19. Traub RD, Pedley TA. Virus-induced electrotonic coupling: Hypothesis on the mechanism of periodic EEG discharges in Creutzfelt-Jakob disease. *Ann. Neurol.* 1981; **10**: 405–410.
20. Foreman B, Mahulikar A, Tadi P *et al*. Generalized periodic discharges and "triphasic waves": A blinded evaluation of inter-rater agreement and clinical significance. *Clin. Neurophysiol.* 2016; **127**: 1073–1080.
21. Shirota Y, Ohtomo R, Hanajima R, Terao Y, Tsutsumi R, Tsuji S. Severely abnormal electroencephalogram in two patients who were treated with cefepime. *Clin. Neurol.* 2012; **52**: 356–359 (in Japanese).
22. Payne LE, Gagnon DJ, Riker RR *et al*. Cefepime-induced neurotoxicity: A systematic review. *Crit. Care* 2017; **21**: 276.
23. Chow KM, Szeto CC, Hui AC, Wong TY, Li PK. Retrospective review of neurotoxicity induced by cefepime and ceftazidime. *Pharmacotherapy* 2003; **23**: 369–373.
24. Sutter R, Rüegg S, Tschudin-Sutter S. Seizures as adverse events of antibiotic drugs: A systematic review. *Neurology* 2015; **85**: 1332–1341.
25. Kaplan PW, Schlattman DK. Comparison of triphasic waves and epileptic discharges in one patient with genetic epilepsy. *J. Clin. Neurophysiol.* 2012; **29**: 458–461.
26. Zeilhofer HU, Benke D, Yevenes GE. Chronic pain states: Pharmacological strategies to restore diminished inhibitory spinal pain control. *Annu. Rev. Pharmacol. Toxicol.* 2012; **52**: 111–133.
27. Jones EA, Weissenborn K. Neurology and the liver. *J. Neurol. Neurosurg. Psychiatry* 1997; **63**: 279–293.
28. Fee C, Banasr M, Sibille E. Somatostatin-positive gamma-aminobutyric acid interneuron deficits in depression: Cortical microcircuit and therapeutic perspectives. *Biol. Psychiatry* 2017; **82**: 549–559.
29. Paz JT, Huguenard JR. Microcircuits and their interactions in epilepsy: Is the focus out of focus? *Nat. Neurosci.* 2015; **18**: 351–359.
30. Kobayakawa Y, Tateishi T, Kawamura N, Doi H, Ohyagi Y, Kira J. A case of immune-mediated encephalopathy showing refractory epilepsy and extensive brain MRI lesions associated with anti-glutamic acid decarboxylase antibody. *Clin. Neurol.* 2010; **50**: 92–97 (in Japanese).
31. Kopczak A, Schumacher AM, Nischwitz S, Kümpfel T, Stalla GK, Auer MK. GAD antibody-associated limbic encephalitis in a young woman with APECED. *Endocrinol. Diabetes Metab. Case Rep.* 2017. https://doi.org/10.1530/EDM-17-0010
32. Kurbatova P, Wendling F, Kaminska A *et al*. Dynamic changes of depolarizing GABA in a computational model of epileptogenic brain: Insight for Dravet syndrome. *Exp. Neurol.* 2016; **283**: 57–72.
33. US Food and Drug Administration. The United States Food and Drug Administration Drug Safety Communication: Cefepime and risk of seizure in patients not receiving dosage adjustments for kidney impairment. [Cited 13 August 2018.] Available from URL: http://www.fda.gov/Drugs/DrugSafety/ucm309661.htm

Supporting information

Additional Supporting Information may be found in the online version of this article at the publisher's web-site:

Figure S1. Graphical abstract.